JPRS-UMS-92-006
31 MARCH 1992

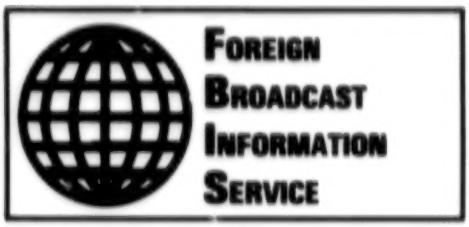

JPRS Report

Science & Technology

Central Eurasia: Materials Science

Science & Technology
Central Eurasia: Materials Science

JPRS-UMS-92-006 CONTENTS 31 March 1992

ANALYSIS, TESTING

CORROSION

FERROUS METALS

NONFERROUS METALS, ALLOYS, BRAZES, SOLDERS

NONMETALLIC MATERIALS

TREATMENTS

WELDING, BRAZING, SOLDERING

EXTRACTIVE METALLURGY, MINING

Substructural Hardening of Aluminum and Its Alloys During Interaction With Gallium

927D0087A Kiev METALLOFIZKA in Russian Vol 13 No 10, Oct 91 pp 3-10

[Article by L.N. Larikov, V.I. Franchuk, and Ye.A. Maksimenko, Institute of Ukrainian Academy of Sciences, Kiev]

UDC 539.2:532.62

[Abstract] An experimental study was made concerning substructural hardening and attendant embrittlement of aluminum and its alloys during their interaction with gallium. Gallium was deposited on aluminum single crystals and on polycrystalline aluminum, also on D6 duralumin and Al-6Mg alloy. Following its deposition at a 297 K temperature, contact between the two materials of each pair was maintained at this temperature over periods of time ranging from a few seconds to 1000 h. Subsequent x-ray structural examination of the substrate materials has yielded data on their texture and lattice parameters as well as on microstresses in them, the Berg-Barret method having been used for tracking the kinetics of substructural changes. The data indicate that diffusion processes attending interaction of aluminum and gallium can cause cracking and fracture as well as substructural hardening of the substrate material, inasmuch as already small amounts of gallium on the boundaries of aluminum grains inhibit their splitting and thus limit shearing action along more and more slip planes. Figures 2; references 24.

Magnetization of Amorphous Alloys by Elastic Deformation

927D0087F Kiev METALLOFIZIKA in Russian Vol 13 No 10, Oct 91 pp 84-91

[Article by V.Ye. Taranichev and M.N. Alenov, Institute of Steel and Alloys, Moscow]

UDC 669.018.583.017.162:539.213.2

[Abstract] An experimental study of two amorphous alloys, strongly magnetostrictive 71Fe-9Co-16B-4Si (λ_s = 30 x 10^{-6}) and weakly magnetostrictive 77Co-12Cr-11Zr (λ_s = 0.7 x 10)$^{-6}$, was made concerning their strain-induced magnetization under pulsed tension. Specimens of both alloys were hardened by quenching the melt and then formed by spinning into 15 cm long and 0.5-2.0 cm wide ribbons. These were placed vertically inside a solenoid in a magnetic displacement field, with the lower end rigidly clamped and the upper end hinged to one arm of a lever beam. The free other arm of the lever was struck by a weight falling from a height of 0.5 cm upon its release from a special impact device. Successively heavier weights were dropped so as to increase the dynamic tensile stress in a ribbon up to 100 MPa. Some ribbons of each alloy were so tested in the quench-hardened state, but of main concern were those tested after they had been annealed in a transverse magnetic field so that their axis of easy magnetization was oriented crosswise perpendicularly to both the external magnetic displacement field and to the direction of mechanical loading. A wire coil wound around each ribbon was connected to an F191 microweber flux meter for magnetization measurements. The earth's magnetic field was compensated for by a permanent magnet. First were plotted two magnetization curves, under zero tension and under static tension, the difference between them representing the dependence of the magnetization increment due to static stress on the magnetic field intensity. Measurements of the magnetization increment due to dynamic stress in a constant external magnetic displacement field, whose intensity was stepwise increased, yielded the dependence of that magnetization increment on the magnetic field intensity. Two almost identical peaking curves were obtained describing the dependence of the magnetization increment due to static stress and due to dynamic stress respectively, both rising steeply to the same maximum magnetization increment at a relatively low magnetic field intensity (within the 1-2.5 A/cm range for the 71Fe-9Cr-16B-4Si alloy) and then falling mildly to zero at a much higher magnetic field intensity (about 20 A/m for the 71Fe-9Cr-16B-4Si alloy). This indicates that, owing to the rotation mechanism activated by annealing in a transverse magnetic field, the final magnitude of magnetization does not depend on the sequence of the external actions: by a mechanical load first or by a magnetizing field first. Thus the dependence of strain-induced magnetization on the mechanical stress in a constant magnetic field follows a saturation curve and its dependence on the magnetic field intensity under a constant mechanical stress follows a peaking curve. This applies to both weakly and strongly magnetostrictive amorphous alloys, strain-induced magnetization of a less magnetostrictive alloy reaching its maximum in a weaker magnetic field and becoming saturated under a higher critical stress. Figures 5; references 9.

Determination of Deformation Profile in Y-Fe Garnet Films After Ion Implantation According to Kinematic Theory of Scattering

927D0086B Kiev METALLOFIZIKA in Russian Vol 13 No 6, Jun 91 pp 102-106

[Article by V.I. Kravets and B.K. Ostafiychuk, State Pedagogical Institute, Ivano-Frankovsk, and S.I. Olikhovskiy, Institute of Metal Physics, UkSSR Academy of Sciences, Kiev]

UDC 548.732

[Abstract] The deformation profile in single crystal Y-Fe garnet films on single crystal Gd-Ga substrates after implantation of low-energy ions is calculated according to the kinematic theory of x-ray scattering. Into such films cut in the (111) plane were implanted 3x10^{14} cm^{-2} 80 keV boron ions or 1.5 x 10^{14} cm^{-2} 80 kev nitrogen

ions or 1 x 10^{14} cm^{-2} 80 keV or oxygen ions or 5 x 10^{14} cm^{-2} 90 keV oxygen ions. Implantation was done with a Vezsuviy-5 apparatus in a configuration which excluded channeling effects. The film with 5 x 10^{14} cm^{-2} oxygen ions was annealed in an oxygen stream at 950°C for 5 h, the other three films were not. All four films were then examined in a two-crystal x-ray diffractometer with a $CuK_{\alpha 1}$-radiation source (copper tube) and a Gd-Ga garnet-crystal monochromator, according to the dispersionless scheme in the symmetric Bragg configuration with reflection in the (444) plane. Diffraction of x-rays by a specimen was measured as the latter was being rotated about its vertical axis so that the angle of incidence of x-rays was varied accordingly. As a result the researchers obtained a curve of diffractive reflection representing the dependence of the intensity of diffracted x-rays on the angle of crystal rotation. With the aid of this curve for a nonpolarized beam of x-rays incident on a crystal-monochromator, the deformation profile in YIG films after ion implantation is calculated upon discretization of such a film into M layers with N atomic planes in each. The calculations are based on the expression for the intensity of waves polarized (p,s) upon diffraction by such a crystal (Z.G. Pinsker; "X-Ray Crystallography", Izdatelstvo Nauka 1982), the intensity of a polarized diffracted wave being proportional to the square of the amplitude of a wave diffracted by a thin deformed layer (Z.G. Pinsker; "X-Ray Crystallography", Izd. Nauka 1982). This amplitude, according to the kinematic theory, equals the sum of the amplitudes of waves reflected by each atomic plane. The calculations have yielded nonmonotonic deformation profiles, evidently owing to existence of an amorphized layer. The deformation profile in the film with 1 x 10^{14} cm^{-2} oxygen ions was found to be similar to those in the films with boron or nitrogen ions. The film with 5 x 10^{14} cm^{-2} oxygen was found to be much less deformed, having been annealed. Annealing had, moreover, transformed its deformation profile into an almost step-like monotonic one, the paramagnetic phase having vanished as a consequence of recrystallization of the amorphized layer. The authors thank V.B. Molodkin for interest and helpful discussions. Figures 1; tables 1; references 10.

Effect of Adding Tin on Dislocation Structure in Copper Single Crystals

927D0087D Kiev METALLOFIZIKA in Russian Vol 13 No 10, Oct 91 pp 59-64

[Article by I.K. Zasimchuk and Ye.P. Pavlova, Institute of Metal Physics, Ukrainian Academy of Science, Kiev]

UDC 548.4'55

[Abstract] An experimental study of Cu single crystals containing tin was made concerning the effect of increasing the Sn content on the dislocation structure in such single crystals grown by a process which would have yielded dislocation-free single crystals of pure copper, tin being dissolvable in copper but with a strong tendency to segregate. Single crystals containing 0.008 atom.% Sn and single crystals containing 0.04 atom.% Sn were grown, some in the [100] direction and some in the [110] direction, under conditions quantifiable in terms of the parameter $f = mc(1 - k_0)v/k_0GD$ characterizing the degree of instability of a plane crystallization front (m = -12 K/atom.% slope of the liquidus line -12 K/atom.%, $k_0 = 0.16$ coefficient characterizing the impurity equilibrium distribution in the melt; c - impurity concentration in the melt; v - velocity of the crystallization front; G - temperature gradient at the crystallization front; D - "impurity in melt" diffusion coefficient). With v = 8.3 μm/s, G = 4 K/cm, and D = 2 x 10^{-5} cm^2/s, the conditions of crystal growth corresponded to $f \approx 5$ for 0.008 atom.% Sn and $f \approx 26$ for 0.04 atom.% Sn. Structural examination of crystal slices was performed under a transmission x-ray microscope. The topograms indicate that increasing the Sn content in Cu single crystals grown under such special conditions from 0.008 atom.% to 0.04 atom.% does not change the randomly disoriented cellular structure into an only slightly disoriented one with an "optimally" developed subgranular one, but rather increases the dislocation density without essentially changing the dislocation pattern. The results are similar to those obtained by increasing the aluminum in Cu single crystals grown under those special conditions but, evidently owing to the much stronger tendency of tin to segregate in copper, they much more closely fit the Tiller- Zasimchuk model of a staircase concentration profile at cell boundaries. Figures 4; tables 1; references 6.

Buildup of Energy and Changes in Microstructure During Deformation of 12Cr18Ni10Ti Steel

927D0087C Kiev METALLOFIZIKA in Russian Vol 13 No 10, Oct 91 pp 36-40

[Article by I.V. Astafyev, O.P. Maksimkin, and B.D. Utkelbayev, Institute of Nuclear Physics, KaSSR Academy of Sciences, Alma-Ata]

UDC 669.1:539.74

[Abstract] The austenitic stainless 12Cr18Ni10Ti steel (0.10 % C, 17.00 % Cr, 10.66 % Ni, 0.50 % Ti, 1.67 % Mn, 0.34 % Si, 0.032 % P, 0.013 % S) was tested for buildup of energy and microstructural changes during deformation. Rods of this steel were rolled into 0.3 mm thick sheets which were then cut in the direction of rolling into strips. From these were stamped out specimens for heat treatment and testing. The heat treatment consisted of heating to 1323 K, soaking at this temperature for 30 min, and cooling in water. The specimens were then elongated at a rate of 0.5 mm/min at room temperature to various strain levels ranging from 3 % to 40 %. The laboratory tensile testing machine included a Calve microcalorimeter. For each specimen were plotted the load-deformation curve and the rate of heat release as a function of time curve. Numerical integration yielded the total work A of deformation and the total

heat dissipation Q, the difference E_s = A-Q being the total energy stored. The structure of specimens was examined under a JEM-100CX transmission electron microscope. An analysis of the data indicates that all load-deformation curves fit the Hollomon stress-strain equation $\sigma = C\varepsilon^n$ and that the 0.2 % yield strength $\sigma_{0.2}$ of the 12Cr18Ni10Ti specimens after heat treatment was close to 20 MPa. The specific total energy stored P = E_s/A was found to depend on the percentage deformation, first increasing proportionally to $(\sigma_i - \sigma_{0.2})^2$ (σ_i- actual stress) from zero to a maximum and then decreasing slowly with further deformation, while the rate of energy buildup was found to increase all the time but first very fast throughout the 0-7 % deformation range and then slower throughout the 7-40 % deformation range. Examination under the electron microscope revealed that the heat treatment of the steel strips had thoroughly annealed them, the dislocation density not exceeding 5 x 10^{12} m^{-2} and particles of the carbide phase not dissolving during the austenitization process. Plastic deformation to a 7 % strain level had increased the dislocation density by almost two orders of magnitude, having also produced packing defects and twins. Further plastic deformation to a 40 % strain level had distorted the crystal lattice so much as to make it impossible to obtain a clear electron diffraction pattern, the estimated dislocation density being higher than 10^{14} m^{-2} and reflections from f.c.c. and h.c.p. lattices being more intense than those from b.c.c. lattices. Figures 3; tables 1; references 4.

Change in Dislocation Structure of Nickel Alloys During Creep

927D0087B METALLOFIZIKA in Russian Vol 13 No 10, Oct 91 pp 22-27

[Article by N.V. Nikulina, L.L. Sorokina, M.P. Uskov, and M.B. Bronfin, Scientific-Industrial Association "VIAM" (All-Union Scientific Research Institute of Aviation Materials), Moscow]

UDC 669.01.620.18

[Abstract] A heat-resistant nickel alloy with a larger than 0.60 volume fraction of γ'-phase was tested for changes in its dislocation structure during creep under tension. Single crystals of this alloy were held under tension, one group under tension along the [001] axis and one group under tension along the [111] axis. Some of each group were held under a stress of 250 N/mm^2 at a 1000°C temperature and some under a stress of 140 N/mm^2 at a 1100°C temperature. After 1-h tests (end of transient creep: 0.6 % deformation along the [001] axis, 0.4 % deformation along the [111] axis) and after 10-h tests (middle of steady creep: 1.5 % deformation along the [001] axis, 1.0 % deformation along the [111] axis), disk specimens were sliced into thin foils for structural examination under a JEM-200CX electron microscope: 1) foils in 001-planes perpendicular and parallel to the [001] axis of crystals which had been under tension along this axis, 2) foils in 001-planes at about the same 54° angle to the [111] axis of crystals which had been under tension along the [111] axis. Analysis of the electron diffraction patterns reveals changes in the structure of γ'-phase precipitates as well as changes in the density and distribution of dislocations along the axes of dendrites and within the interaxial spaces. The dislocation density was calculated by the method of secants, accurately within about 10 %. The results indicate an accelerating coalescence of γ'-phase particles, which lowers the stability of the two-phase structure, and a decreasing dislocation density. The interaxial spaces in a single crystal of this alloy are consequently sites of a decreasing resistance to creep. The dislocation structure was, moreover, found to evolve differently under tension along the [001] axis and under tension along the [111] axis. In the latter case the dislocation density was lower, in accordance with the Shmid factor. Figures 4; tables 2; references 4.

Use of Interactive Graphical System "Refleks" for Analysis of Pinhole Electron Diffraction Micropatterns Under Transmission Electron Microscope

927D0087E Kiev METALLOFIZIKA in Russian Vol 13 No 10, Oct 91 pp 65-69

[Article by G.M. Grigorenko, A.V. Tayanovskaya, and P.I. Tayanovskiy, Institute of Electric Welding, Ukrainian Academy of Sciences, Kiev]

UDC 620.187.3

[Abstract] Use of a programmable computer such as the IBM P/C AT type for decoding pinhole electron diffraction micropatterns under by the Ewald method of lattice calculations is proposed, the interactive graphical "Refleks" system developed for this purpose including software written in the TURBO PASCAL programming language and a PRODIS deck of punch cards. The algorithm of phase identification by this method is based on three premises: 1) Owing to interference of scattered waves, atomic planes separated by a distance d can reflect a wave of length λ only in the direction which satisfies the Wolf-Bragg condition $2d\sin\theta = n\lambda$ (θ - angle between wave vectors K_0 and K_D referring to the incident wave and to the wave diffracted by an atomic plane respectively; n - integer); 2) Rotation of the crystal specimen will be exactly duplicated by rotation of the reciprocal lattice about its null node while its hkl node will move inside or outside the reflection sphere whose center is the common origin of both wave vectors and whose radius is equal to their length $|K| = 1/\lambda$ in the wave-vector space (such a change of crystal orientation, or a change of the interplanar distance without change of crystal orientation, violates the Wolf-Bragg condition and, therefore, and no diffraction of an electron beam will take place); 3) For fast electrons used in transmission electron microscopes ($\lambda \leq 0.004$ nm) the radius of this reflection sphere is much longer than the internodal distance in the reciprocal lattice so that some segment of

the sphere around the null node may be regarded as an approximately plane one. According to this scheme, the direction of propagation diffracted electron beams in the real space inside the diffraction chamber will be the same as in the wave-vector space. Inasmuch as the scale of diffraction patterns is determined by the distance L from the specimen to the screen or photographic plate, the product λL must be held constant in a diffraction chamber of fixed length when the accelerating voltage is also fixed. Operation of the "Reflex" system is demonstrated on computer simulation of electron diffractograms of crystals with f.c.c. and b.c.c. lattices. The menu entries are: RISEGRAM construction of theoretical electron diffractogram; UGL X clockwise rotation of crystal about X-axis; UGL-X counterclockwise rotation of crystal about X-axis; UGL Y clockwise rotation of crystal about Y-axis; UGL-Y counterclockwise rotation of crystal about Y-axis; END exit from system; REFRAD select radius of reflection sphere; VVOD input of experimental data. Figures 2; references 3.

X-Ray Diffraction Analysis of Molten Eutectic Ni-Ta Alloy

927D0086D METALLOFIZIKA in Russian Vol 13 No 6, Jun 91 pp 116-129

[Article by L.Ye. Mikhaylova, A.V. Romanova, and A.G. Ilinskiy, Institute of Metal Physics, UkSSR Academy of Sciences, Kiev, and Chen SiShen, Institute of Physics Academy of Sciences of People's Republic of China, Beijing]

UDC 532.74:539.213:549.2

[Abstract] An x-ray diffraction analysis of the eutectic alloy Ni + 37.5 atom.% Ta in the molten state at 1700°C (melting point 1332°C) was performed for a study of its structure, this alloy having been produced from 99.99 % pure nickel and tantalum with 4 wt. % W by the electric-arc process with a nonconsumable tungsten electrode in an argon atmosphere. Measurements were made in a high-temperature x-ray diffractometer with a MoK_{α}- radiation source and a graphite monochromator. The high-tempeature chamber contained helium under a gage pressure of about 1 atm. The scattering angle 2θ was increased up to 50°. First a film of the tetragonal crystalline TaO_2 oxide was found to cover the melt surface at 1340-1590°C, this film beginning to disappear rapidly at 1570°C already. An x-ray fluorescence analysis performed in an MS-46 diffractometer at 1700°C revealed that another surface film, of Ta_2O_3 and Al_2O_3 oxides, had covered the melt as the latter was being held at this temperature for a lengthy period of time. An analysis of the data indicates that they do not fit the single-structure model based on the statistics of atom distribution and interatomic distances, but admit interpretation on the basis of a two-structure model. Several such models are considered, further calculations indicating that the melt of this Ni-Ta alloy has a nonhomogeneous microstructure even at a temperature about 400°C above its melting point. According to the best fitting model, two kinds of microclusters like those in the Ni_3Ta phase have formed in this melt with short-range orders different than those in the crystalline Ni_2 and NiTa phases forming during uniform crystallization of the eutectic alloy. Microclusters of the first kind contain preferentially Ta atoms in a crystal lattice similar to a b.c.c. one each, with a 10.6 mean-weighted coordination number. In microclusters of the second kind Ta atoms are surrounded preferentially by Ni atoms forming a short-range order with a mean coordination number 12, while a Ni atom is surrounded by eight Ni atoms and four Ta atoms. The structure of amorphous eutectic Ni-Ta alloy produced by fast cooling of the melt is, according to this model, quite similar to that of the melt. Figures 3; tables 4; references 24.

Peculiarities of Electrical and Magnetoelectrical Properties and of Microstructure of Permalloy Films

927D0086C Kiev METALLOFIZIKA Vol 13 No 6, Jun 91 pp 107-115

[Article by V.O. Vaskovskiy, G.S. Kandaurova, V.N. Lepalovskiy, A.N. Sorokin, Ye.I. Teytel, and N.N. Shchegoleva, Ural State University, Sverdlovsk]

UDC 539.216; 539.213

[Abstract] Films of 19Fe-81Ni and 10Fe-90Ni Permalloys produced by ion sputtering were tested for electrical resistivity ρ and magnetoresistivity anisotropy $\Delta\rho$ after thermomagnetic treatment. From the entire Permalloy series the 10Fe-90Ni material was selected on account of the strongest magnetoresistance effect, while the 19Fe-81Ni material was selected because of its smallest coercive force owing to both weakest magnetostriction and weakest crystallographic-magnetic anisotropy. After the 45+/-5 nm films of both materials had been deposited on single crystal Si(001) substrate plates by high-frequency ion sputtering in a parallel magnetic field of 8 kA/m intensity, with the temperature of the substrates maintained at 200°C, they were annealed by thermomagnetic treatment without loss of vacuum (0.2 mPa) at various temperatures ranging from 200°C to 600°C in a magnetic field of given orientation and intensity. The treatment continued for 1 h, sufficiently long for stabilizing the properties of the films after complete relaxation. Microstructural examination of the films was performed in a DRON-UM1 x-ray diffractometer with a CrK_{α}-radiation source and three slits respectively 0.5 mm, 0.5, and 1.0 mm wide, the (110) line being used for analysis. It was also performed under a JEM-200CX electron microscope, with a Permalloy film on a (001)-cut NaCl substrate crystal serving as reference standard. The results indicate the effect of thermomagnetic treatment on both the electrical resistivity and the magnetoresistivity anisotropy of Permalloy films, including the dependence of these properties as well as of the grain size on the treatment temperature. The changes of both electrical

resistivity and magnetoresistivity anisotropy caused by thermomagnetic treatment are evidently manifestations of microstructural transformations attributable not only to magnetization but also to film-substrate interaction, these transformations resulting in change of the intragranular and intergranular defectiveness pattern as well as in change of the mean grain dimension and in formation of secondary phases. The authors thank A.V. Andreyev for performing the x-ray spectroscopy of films. Figures 7; references 11.

Integral Intensity of Diffuse Scattering of X-rays During Anomalous Passage Through Crystals With Microdefects

927D0086A Kiev METALLOFIZIKA in Russian Vol 13 No 6, Jun 91 pp 84-91

[Article by V.V. Kochelab, V.B. Molodkin, and S.I. Olikhovskiy, Institute of Metal Physics, UkSSR Academy of Sciences, Kiev]

UDC 639 26:548.4

[Abstract] Diffuse scattering of x-rays during their anomalous passage through a single crystal containing microdefects of any kind is analyzed in the approximation of thick crystal, assuming a random distribution of the microdefects over the crystal volume. The average distortion of the crystal is moreover assumed to be weak ($L << 1$), the characteristic dimension of the microdefects being much smaller than the x-ray extinction length. The integral intensity of diffuse scattering is calculated on the premise that the total diffuse and Bragg integral scattering intensity depends only on two parameters characterizing the degree of structural perfection of a crystal: distortion index L and constant $\mu_{d_0}{}^0$ characterizing the microdefects ($\mu_{d_0}(y)$ - Dederich coefficient of absorption of diffusely scattered x-rays, dependent on the deviation y of the direction of x-ray incidence from the exact Bragg angle in the plane of scattering). Thermal diffuse scattering is assumed to make only a negligible direct contribution to the total diffuse scattering, but the Debye-Waller factor is implicitly included in the structural factor characterizing a perfect crystal. An expression for the diffuse scattering component R_D' of the integral scattering coefficient and its dependence on the thickness of the crystal is derived from the expression for the diffuse scattering coefficient R_Dk characterizing a single crystal with randomly distributed microdefects in a symmetric Laue diffraction pattern, integration being performed in the k-space. This derivation is aided by use of the asymptotic expression for the coherent component of the integral scattering coefficient (Z.G. Pinsker; "X-Ray Crystallography", Izd. Nauka 1982), with corrections for the Fourier components of polarizability in an imperfect crystal, specifically one with Coulomb microdefects. The authors thank M.Ye. Osinovskiy for helpful discussion. References 13.

Unit for Composite Material Torsion Tests at Temperatures of Up to 3,300K

927D0124I Kiev PROBLEMY PROCHNOSTI in Russian No 1(271), Jan 92 pp 87-88

[Article by A.V. Bogomolov, V.A. Borisenko, Strength Problems Institute at the Ukrainian Academy of Sciences, Kiev]

UDC 620.1.05.052

[Abstract] The need to assess the transversal and shear characteristics of composite materials prompted the development of a unit for high-temperature mechanical testing; the unit developed at the Ivanovo "Tochpribor" Production Association on the basis of the 2014 MK-50 torsion testing machine contains a vacuum chamber with a heating system and devices for measuring torque and the twist angle in a vacuum and in inert gas media. The unit makes it possible to predict the behavior of composite materials under torsion at temperatures of up to 3,300K and the development of such defects as lamination, porosity, and cracks. A block diagram of the new twist testing unit and its photograph are shown. Figures 2; references 3.

Interrelation of Rotating Stall and Blading Vibrations

927D0124H Kiev PROBLEMY PROCHNOSTI in Russian No 1(271), Jan 92 pp 82-87

[Article by N.P. Aleshin, Progress Mechanical Engineering and Design Office, Zaporozhye]

UDC 621.51:534.1

[Abstract] The community of properties of the rotating stall and blading vibrations in the form of traveling deformation waves prompted a search for the specific relationship between these phenomena; in so doing, the outcome of experimental studies and design features of eight supersonic compressors are considered and pressure fluctuation oscillograms in the compressor setting and variable strain diagrams of the individual blades plotted under rotating stall conditions are analyzed. Two multistage axial compressors, one single-stage transsonic fan, and five fan modifications are examined. The study confirms the existence of a link between the rotating stall and the blading vibrations whereby the stall zones generate and maintain the blading vibrations which are realized as traveling deformation waves which, in turn, are captured by the deformation waves and transferred along the blading circumference. The above findings were presented to the Eleventh All-Union Conference on Aeroelasticity of Machines. Figures 5; references 6.

Characteristics of Composite Material Obstacle Perforation by Strikers of Various Shapes

927D0124G Kiev PROBLEMY PROCHNOSTI in Russian No 1(271), Jan 92 pp 60-62

[Article by V.P. Muzychenko, M.A. Drozdov, V.I. Shlyakhov, All-Union Scientific Research Center on the Problems of Shock and Failure, Riga and Daugavpils]

UDC 534.26+539.374

[Abstract] Perforation curves which connect critical puncture velocities to the parameters of the strikers and obstacles are discussed and the results of ballistic tests of obstacles from composite materials perforated by strikers of various shapes are presented in the form of such curves. The dependence of the projectile velocity at the point of exit on the projectile velocity at the point of entry for the KITE-70 composite material perforated by strikers of various shapes, the dependence of the projectile velocity drop on the projectile velocity at the point of entry, and the puncture resistance of the KITE-70 material in the postcritical area under impact loading by strikers of various shapes are examined and plotted. An analysis of the findings shows that the striker shape, overall dimensions, and mass affect not only the quantitative aspect of the perforation characteristics of composite materials manifested in a change in their critical perforation velocities but also their qualitative aspect. Figures 3; references 5: 2 Russian, 3 Western.

Method of Electric Simulation of Contact Stresses During Indentation of Eccentrically Loaded Punch Shaped as Paraboloid of Revolution Into Elastic Half-Space

927D0124F Kiev PROBLEMY PROCHNOSTI in Russian No 1(271), Jan 92 pp 57-60

[Article by G.P. Tarikov, Gomel Polytechnic Institute]

UDC 539.319.001.57

[Abstract] The importance of solving spatial contact problems for the purpose of strength analysis of machines and mechanisms is stressed and an experimental solution of such a problem is considered in the case where the shape of the contact area and the contact stress distribution law differ from classical. To this end, a punch shaped as a paraboloid of revolution is indented into an isotropic elastic half-space under the effect of an offset force. The possibility of solving the problem by the method of electric simulation is demonstrated and the experimental error is estimated and compared to the theoretical findings. An analogy between the equations describing the distribution of reaction pressure on the contact area and the electric charge distribution on the surface of a conducting slab is noted and a procedure for solving the indentation problem with the help of a special electric simulator is proposed. Indentation of a second-degree paraboloid punch is considered for illustration and the effect of the punch slope on the reaction pressure distribution on the contact area is investigated. Reaction pressure distribution profiles are plotted. It is shown that the proposed electric simulation method may also be used for determining the punch travel and rotation angle as well as solving more complicated spatial contact problems. Figures 2; tables 1; references 5.

Plotting *R*-Curves for Ceramics

927D0124E Kiev PROBLEMY PROCHNOSTI in Russian No 1(271), Jan 92 pp 36-42

[Article by V.P. Zavada, Strength Problems Institute at the Ukrainian Academy of Sciences, Kiev]

UDC 539.375+666.76

[Abstract] The importance of assessing the crack resistance of ceramics used for crucial structural members is discussed and a technique of examining the ceramics *R*-curves is described; prismatic samples with a notch (stress concentrator) between two supports are studied under concentrated force bending. A crack was either grown beforehand from this notch by combining axial bending with compression or by slowly loading the sample under bending conditions. Samples with a crack display a nonlinearity and hysteresis in the load-sag diagrams as well as a residual defection after the load is relieved. This phenomenon is attributed to friction between the crack edges. A model is proposed for estimating the effect of the friction force on crack resistance and for taking it into account. Both single- and multisample methods are used to plot the *R*-curves, i.e., the dependence of K^{*}_{1c} on the crack length. The sample cracking is determined by the acoustic emission (AE) method. It is emphasized that although more detailed data on the character of friction forces and their behavior during the crack nucleation and propagation are needed, available results convincingly attest to the presence of such forces and make it possible to consider them as one of the causes of the *R*-curve manifestation in ceramics due to an increase in the interaction surface of the crack edges during the crack growth. The author is grateful to A.I. Fesenko for help with the experiment and G.A. Gogotsi for discussing the findings. Figures 5; tables 1; references 10: 5 Russian, 5 Western.

Effect of Annealing Conditions on Formation of Structure and Its Correlation With Mechanical Properties of Al-Be Alloy Foils

927D0124D Kiev PROBLEMY PROCHNOSTI in Russian No 1(271), Jan 92 pp 28-32

[Article by L.I. Kolesnik, K.V. Oleynikov, P.M. Romanko, V.G. Tkachenko, Yu.V. Usov, Institute of Materials Science Problems at the Ukrainian Academy of Sciences, Kiev]

UDC 620.18:620.17:669.71'725

[Abstract] The patterns of structure formation of aluminum-beryllium alloy foils after annealing are investigated; to this end, the effect of the annealing temperature and duration and their combination on the mechanical properties—the yield strength, ultimate strength, and elongation—of aluminum and beryllium foils is examined under uniaxial tension using a 1231 machine. The effect of annealing on the aluminum and beryllium components of the alloy is established and the methods of mathematical rotatable experiment design are used to derive the dependence of the mechanical properties on the annealing temperature and duration as well as the effect of structural parameters on the foils' mechanical properties. A disperse cellular structure with a high matrix dislocation density develops in the alloy's Al-component under the effect of intensive plastic deformation by rolling. A decrease in the foils' yield strength is described by the Hall-Patch formula and is controlled by the cellular structure size of the Al-component. The study reveals that foils fail in two stages: first, the reinforcing Be particle fails by the brittle spalling mechanism; then the alloy matrix fails by the viscous mechanism. Figures 7; tables 1; references 15: 12 Russian, 3 Western.

Effect of Low-Intensity Impulse Loading on Mechanical Characteristics of Steels 20 and 12Kh19N10T

927D0124C Kiev PROBLEMY PROCHNOSTI in Russian No 1(271), Jan 92 pp 23-27

[Article by A.V. Maslakov, Strength Problems Institute at the Ukrainian Academy of Sciences, Kiev]

UDC 539.4+539.214:620.171.31

[Abstract] The effect of low-intensity pulse loading on samples punched from sheets of steels 20 and 12Kh18N10T with a visible rolling texture with an orientation across and along the rolling direction is examined. The tensile strain diagrams of the above steel samples and the behavior of their relative yield strength, ultimate strength, and elongation is investigated and plotted. Quasistatic uniaxial tension tests are carried out on short proportional samples cut from the sheets pulse-treated at a pressure of under 2 GPa. The results show that the change in mechanical properties of these structural steels depends on the strain developing under the low-intensity pulse loading and that low pulse deformations of under 1% lead to a sharp increase (by close to 30%) in the yield strength of steel 12Kh18N10T. As the pulse strain increases to 8%, the percentage reduction of area decreases somewhat while the reduction of area at fracture decreases by approximately twofold. The yield site on the strain diagram of steel 20 which is typical of this material disappears as a result of the pulse loading treatment. Figures 4; tables 1; references 10.

Temperature Dependence Anomaly of Austenitic and Transition Steel Elasticity Moduli

927D0124B Kiev PROBLEMY PROCHNOSTI in Russian No 1(271), Jan 92 pp 20-23

[Article by A.F. Voytenko, Strength Problems Institute at the Ukrainian Academy of Sciences, Kiev]

UDC 539.53

[Abstract] The temperature dependence of the modulus of elongation of Fe-Mn alloys and steel 03Kh13AG19, the behavior of resonance frequency and sag of steel 03Kh13AG19 with a decrease in temperature, the effect of temperature on the mechanical properties of steel 03Kh13AG19, and the temperature dependence of the modulus of elongation of austenitic steels 12Kh18N10T, 05Kh20N10AG10, 03Kh20N16AG6, 07Kh13N4AG20, and 03Kh13AG19 as well as steels KH12N2VMF, 07Kh16N6, 02Kh13GN9MDF1, and 0M9 are examined and plotted. The results reveal that for austenitic and transition steels, the modulus of elongation does not increase with a decrease in temperature within certain temperature ranges but decreases. This anomaly occurs in commercial steels with 10% or more of austenite and its magnitude depends on the austenite's chemical composition. It is also noted that chromium, an antiferromagnetic material, substantially lowers the above anomaly of the elongation modulus's temperature dependence. The anomaly is attributed to an antiferromagnetic ordering in austenite. The importance of investigating this anomaly—which occurs within a temperature range in which mechanical properties change in transition, martensitic, austenitic, and ferritic steels—is emphasized. Figures 5; references 5.

Thermal Stability of Ti-W Hard Alloys

927D0124A Kiev PROBLEMY PROCHNOSTI in Russian No 1(271), Jan 92 pp 13-16

[Article by G.I. Chepovetskiy, T.E. Gracheva, L.M. Tsirinskaya, Superhard Materials Institute at the Ukrainian Academy of Sciences, Kiev]

UDC 620.171.32:669.018.25

[Abstract] The advantages of titanium-tungsten hard alloys used as tool materials are discussed and an attempt to measure the thermal shock resistance of Ti-W hard alloys and the hard alloys' residual strength at various thermal shock temperatures is reported. Commercial (Ti,W)C-WC-Co alloys which are a three-phase material consisting of a binary carbide solution of titanium and tungsten—the T15K6 and T5K10—are used in the experiments which show that the former alloy has a critical thermal shock temperature of 400°C while the latter has a 500°C critical temperature characterizing the material's heat resistance. The statistical characteristics of the experimental residual strength data are examined and an increase in the residual strength of the T5K10

alloy at a 700°C thermal shock temperature is attributed to its proximity to the viscobrittle transition temperature of this alloy which has a higher proportion of the binding phase. It is recommended that the T5K10 alloy be hardened by heat treatment. It is also noted that the heat resistance of Ti-W alloys is lower than that of hard tungsten alloys by about twofold. Figures 3; references 11: 8 Russian, 3 Western.

The Corrosion Resistance of 20895 Electrical Steel With a Chrome-Plated Coating

927D0105B Moscow METALLOVEDENIYE I TERMICHESKAYA OBRABOTKA METALLOV in Russian No 11, Nov 91 pp 4-6

[Article by S.G. Babich, A.A. Zyabrev, G.V. Skibina, and N.V. Vavilova, Physicochemical Institute imeni L.Ya. Karpov and Moscow State Technical School imeni N.E. Bauman]

UDC 620.193:621.785.539:669.018.5

[Abstract] Magnetically soft 20895 electrical steel (0.035% C, 0.30% Mn, 0.30% Si, 0.20% P, 0.020% S, and 0.030% Cu) was subjected to chrome plating by the circulation method in chloride gas medium at temperatures of 950 and 1,000°C for 1 to 9 hours in order to protect it against corrosion. The circulation saturation of the steel's surface was performed as follows. A muffle holding the components and saturating substance (chromium granules) was heated to the diffusion saturation point and then filled with the chloride gas. A ventilator was turned on, and the muffle was held for specified amounts of time and then cooled at set rates. After the components had been loaded, the muffle was evacuated to P = 13.3. Pa. The gases were continually pumped from the chamber while the components were heated and cooled. The quality of the chrome-plated surfaces was determined by metallographic, x-ray, potentiostatic, and atomic-absorption methods. The microhardness of the surface layer of the test specimens was measured, and they were subjected to corrosion tests in a humid atmosphere for 6 months. The studies performed revealed that the thickness of the chromized layer increased as the chrome-plated temperature and holding time were increased. The structure of the outer part of the surface layer was found to consist of an α-solid solution of chromium in Fe_α, traces of carbides based on chromium of the $M_{23}C_6$ and M_7C_3 type, and a σ-phase (FeCr). The structure of the inner part of the coating was found to be an α-solid solution. The microhardness of the surface of specimens chrome-plated at 1,000°C for 3 hours was found to be 240 HV, whereas the microhardness in the center of the components tested was found to be 160 HV. Those test specimens that were chrome-plated at 950°C for 9 hours and at 1,000°C for 3 hours were found to have the greatest corrosion resistance in a 3% aqueous solution of NaCl. Specimens chrome-plated at 950°C for 9 hours were found to have a corrosion current at a potential of 0.5 V that was three orders of magnitude below specimens chrome-plated at the same temperature for 1 hour and five orders of magnitude below that of steel without a chrome coating. Steel specimens chrome-plated at 1,000°C for 3 hours had the lowest corrosion current of all. Comparative tests indicated that 20895 chrome-plated electrical steel is far more corrosion resistant than Cr18 steel. The chromeplating regimen tested was found to induce a high degree of corrosion resistance in corrosive media within a broad range of oxidizing-reducing media as well as under atmospheric conditions. It was also found to result in a reduction in coercive force, which is especially important for magnetically soft alloys. Figures 2, table 1.

High-Damping Cr-Al Steel

927D0105G Moscow METALLOVEDENIYE I TERMICHESKAYA OBRABOTKA METALLOV in Russian No 11, Nov 91 pp 44-45

[Article by A.I. Skvortsov and V.M. Kondratov, Kirov Polytechnic Institute]

UDC 669.14.018.6

[Abstract] The authors of the study examined the damping and mechanical properties of type 04Kh11Yu steel with an aluminum content of 0.02 to 3.9%. Test specimens of four types of the said steels (04Kh11, 04Kh11Yu, 04Kh11Yu3, and 04Kh11Yu4) were examined after annealing at 850 and 1,050°C. The said steels each contained about 11% chromium (10.7, 10.5, 10.8, and 10.7%, respectively) and approximately the same amounts of carbon (0.04, 0.05, 0.04, and 0.05%, respectively) but different amounts of aluminum (0.02, 0.50, 2.75, and 3.90%, respectively). The steels were smelted in an open induction furnace from commercial-grade materials. Castings were forged into bars 16 mm in diameter or with a cross section of 13 x 13 mm and were then subjected to annealing at either 850 or 1,050°C. The experiments conducted confirmed that damping depends both on aluminum content and annealing temperature. In the case of annealing at 850°C, the maximum damping was found in the steels containing between 0.5 and 2.8% aluminum. In the case of annealing at 1,050°C, the maximum damping was found in specimens containing close to 3% aluminum. This increase in damping was explained in terms of the magnetomechanical hysteresis of iron when it is doped with aluminum. Structural defects formed during ordering of the α-solid solution analogous to ordering in high-silicon steel was deemed the likely cause of the reduction in damping with increased aluminum content. The 04Kh11Yu specimens were found to have the maximum damping capability (16%) after annealing at 850°C. The steels containing 0.5 to 4% aluminum were found to have a high resilience and satisfactory strength. The studies thus indicated that to achieve high damping and good workability, type 04Kh11 should be doped with 0.5 to 3% aluminum. Figures 3, table 1; references 5 (Russian).

Temperature Conditions in Flash Melting Furnace

927D0030A Moscow TSVETNYYE METALLY in Russian No 6, Jun 91 pp 19-22

[Article by V.V. Kobakhidze, L.D. Talis, A.A. Kazhdan, G.V. Indenbaum, and B.M. Boynykh, Moscow Institute of Steel and Alloys]

UDC 669.2.8.041:621.1.002.56

[Abstract] Aerodynamic and temperature conditions in a flash melting furnace of the NG State Metallurgical Combine producing copper and Cu-Ni matte concentrates were studied with the furnace in the moderate operating mode: charging rate 120 t/h, 40-50 % oxygen enrichment, blast rate 55,000 m^3/h. In this mode the furnace produced matte containing about 25 % Ni and about 13 % Cu at four levels in the vertical reaction shaft with lined wall. Boundaries of the flame flow zone were established by measurements with a Pitot tube and sampling of specimens with a crowbar. Specimens of the reaction product in the shaft were transferred to a water-cooled sampler for mineralogical analysis. The flux density of intrinsic radiation emission by the gas-burden flame was measured with a radiometer. Temperatures inside the reactor shaft and in the gaseous region of the sump were measured with a water-cooled thermocouple. The gas-burden flame was found not to occupy the entire volume of the reaction shaft, a recirculation zone with a low concentration of solid particles forming along the entire shaft height. The results of mineralogical analysis performed on polished unetched specimens under a Neophot-21 reflection microscope indicate that the composition of the burden changes increasingly downward along the shaft and from the central region toward the periphery of the flame, the high-temperature zone of intense oxidation of sulfides meanwhile spreading from the periphery toward the center of the shaft and from its upper region downward. The pressure measurements revealed 30-50 Pa wide pressure fluctuations within both flow and circulation zones of the flame and an approximately 100 Pa pressure jump at the crossover from one zone to the other. The temperatures in this flash melting furnace are compared with those in an oxygen-flame melting furnace of the AG State Metallurgical Combine (V.V. Kobakhidze, A.A. Kazhdan, and V.Z. Kalach; TSVETNYYE METALLY No 11, Nov 88), both furnaces being of the hybrid type and both found to have to have a highly nonuniform temperature distribution. The temperature of the gas exceeds the mean surface temperature of solid particles throughout almost the entire flame, but their temperatures tend to equalize within the uptake region. As in the case of oxygen-flame melting furnaces, therefore, the performance of flash melting furnaces can be improved by ensuring a better heat transfer within the gas-burden flame so that the burden in gaseous suspension will be more thoroughly processed with less waste of metal and slag. Figures 4; tables 1; references 4.

The Durability of Structurally Stable Nickel Alloys

927D0105D Moscow METALLOVEDENIYE I TERMICHESKAYA OBRABOTKA METALLOV in Russian No 11, Nov 91 pp 13-15

[Article by I.I. Trunin, S.A. Yuganovam, and Yu.V. Kashirskiy, Central Scientific Research Institute of Machine Building Technology Scientific Production Association]

UDC 669.14.018:44:620.178.3

[Abstract] The authors of this article have performed a mathematical analysis of the destructive processes occurring during the creep of alloys. A formula is derived for use in determining the durability of refractory nickel alloys. The correctness of the formula was verified on the basis of experimental data published in the literature. Specifically, the authors cite research indicating that the effect of phase composition and structure of refractory properties of nickel alloys of the system Ni-Cr-Al-Ti is linked to four factors that are taken into account in the formula presented. These factors are as follows: 1) the amount of aluminum and titanium (which affects the interatomic bonding forces of the matrix); 2) the content of aluminum and titanium in the solid solution (which is reduced as a result of separation of the γ'-phase, thus resulting in an increase in the interatomic bond forces in the matrix); 3) the aluminum:titanium ratio in the alloy (which determines the degree of concentration of stresses at the interface); and 4) the size of the particles of the γ'-phase (which affects the laws governing the accumulation of plastic deformation and damages). The first two factors, which affect the activation energy of fracture during creep, are taken into account by two terms in the expression presented. These two terms represent the sum of the atomic fractions of aluminum and titanium in the γ-phase and the amount of γ'-phase. The third and fourth factors are expressed by the introduction of two correcting factors. Tables 3; references 6 (Russian)

Calculating Rapid Oriented Crystallization Modes

927D0103E Moscow LITEYNOYE PROIZVODSTVO in Russian No 10, Oct 91 pp 29-30

[Article by M.M. Koroleva and S.V. Lobanov, Rybinsk Aviation Technology Institute]

UDC 621.74:681.3

[Abstract] A new application package has been developed for use in calculating rapid oriented crystallization modes. The new application package is based on a unidimensional mathematical model of rapid oriented crystallization that establishes a time link between the key process parameters and their dependence on casting conditions and the geometry and materials of the casting, ceramic mold, and ceramic inner core. The mathematical model of rapid oriented crystallization on

which the application package is based has been implemented by the finite differences method. In essence, a casting with a length of *L* is divided into a set of *I* elements. The following basic and auxiliary arrays are determined: *TI* (the array of ongoing temperatures), *QI* (the array of ongoing heat contents); *QLI* (the array of heat fluxes along the length of the casting), *QRI* (the array of radial heat fluxes through the wall of the casting mold); *NFI* (the array of phase numbers [which specifies the aggregate state of a casting element at the current moment in time]); and *NZI* (the array of zone numbers [i.e., the zones of the casting unit through which the casting passes during the casting process, including the crystallization furnace, heat screen, and molten metal cooler]). The authors detail the five steps followed to calculate these arrays. The new application package makes it possible to design rapid oriented crystallization modes that will prevent the formation of various structural defects in castings. The new application package may also be used as software in existing automated technological process control systems.

An Application Package To Design Investment-Pattern Casting Processes

927D0103D Moscow LITEYNOYE PROIZVODSTVO in Russian No 10, Oct 91 p 15

[Article by A.F. Smykov, V.I. Dankov, and S.V. Modin, Moscow Aviation Technology Institute imeni K.E. Tsiolkovskiy]

UDC 621.74.045.001.63:681.3

[Abstract] A new application package to design processes to manufacture steel castings based on the investment-pattern casting technique has been developed at the Moscow Aviation Technology Institute imeni K.E. Tsiolkovskiy. The new application package makes it possible to automate the configuration of casting units and computation of the following: the temperature at which metal is to be poured into the mold; the sequence in which the elements in a unit solidify; the dimensions of the central sprue and the horizontal and vertical collectors, and local sinkheads and feeding gates. The new application package also makes it possible to formulate process documentation. The casting unit configuration method used in the application package is based on the principle of structural optimization with an allowance for industrial experience and existing technological recommendations. Castings are configured in a unit based on a casting and feeding gate system selected by the designer. The program to formulate process documentation has been designed so that the documentation generated will conform to the specifications of existing pertinent All-Union State Standards (specifically GOST 3.1401-86 and GOST 3.1118-82). Documents developed by using the application package may be stored, retrieved from archives, and printed out. The application package is geared toward use on IBM PC's and is intended to be used interactively. The individual programs in the package may be used individually or as a unified system.

Computerization of Computations To Obtain Titanium Castings

927D0103C Moscow LITEYNOYE PROIZVODSTVO in Russian No 10, Oct 91 pp 13-14

[Article by A.A. Neustruyev, V.S. Moiseyev, Moscow Aviation Technology Institute imeni K.E. Tsiolkovskiy, and G.L. Khodorovskiy, Aviation Technology Scientific Research Institute]

UDC 621.74.681.3

[Abstract] The main method of manufacturing shaped titanium castings is that of centrifugal casting with a vertical mold rotation axis. In the case of centrifugal casting, the casting is considered to consist of N elements with simple configurations (parallelepiped, cylinder, prism, etc.) because the flow of melt in the mold and centrifugation of the solid phase depend on the geometry and relative arrangement of these elements in the casting. Such computations can only be made by computer. Two computer programs—one to calculate the filling of the mold with the melt and one to calculate solidification of the casting—are central to the process of computing the computations required when producing titanium castings by the centrifugal casting technique. Two gate systems are currently used to produce titanium castings by the centrifugal casting method, namely, systems in which the runner is above the casting and systems in which it is located below the casting. A program has been developed that permits users of IBM-type PC's to perform the calculations required to design a process using either gate system. Specifically, the new programs make it possible to design casting processes with consideration for the following facts: 1) the rapid cooling of a casting results in large temperature differentials throughout its nodes, 2) from the moment the mold comes into contact with the molten metal being pored into it, a solid metal skin forms that subsequently grows and fuses, and 3) the centrifugation of the bulk-hardening solid phase in a casting's elements exert a significant effect on the casting process in the solidification stage. The calculations may be performed in an interactive mode. Using the new computer programs enables casting process designers to reduce the use of scarce and expensive titanium alloys in gate and feed systems. The new programs may also be used to debug processes being designed to produce new and especially complex blanks. Figures 4, references 4 (Russian).

The Use of Pulsed Lasers To Measure the Thermal Properties of Molding Mixtures

927D0103B Moscow LITEYNOYE PROIZVODSTVO in Russian No 10, Oct 91 pp 8-9

[Article by Zang Jiayu and Yang Hua [phonetics], People's Republic of China]

UDC 621.742.42

[Abstract] The authors of the study used pulsed lasers to measure the processes of shrinkage and pore formation in castings as they cool and solidify. First, they derived a series of expressions that could be used with their pulsed laser technique to calculate the temperature conduction coefficient, heat capacity, and heat conduction of molding mixtures. For their studies, they used a ruby laser powered by a xenon lamp. The laser's body was in the shape of a rod 12 x 310 mm. A heating furnace stack was used to create temperatures of ≤1,500°C. The laser pulse was absorbed by the face surface of the test specimens, thereby generating a process of temperature increase on the opposite surface. The increase in temperature of the rear surface was established by using a thermocouple or infrared radiometer, and the data were written into the memory of a PC after 1,500x amplification. A microprocessor was used to process the measurement data and results. Test specimens measuring 10 x 3 mm of three sand mixtures (quartz, chromite, and corundum) and of types 70 and S2 molding mixtures were used. The chromite, type S2, corundum, and type 70 mixtures all had a higher heat conduction than did the mixture based on quartz sand. The corundum and type 70 mixtures had a higher heat capacity than the other mixtures tested, thus confirming that they absorb heat better than their counterparts. From the standpoint of thermophysical parameters, the corundum and S2 mixtures may replace the chromite mixture as a facing material for large steel castings. Figures 2; references 5 (Russian).

The Poligon Application Package To Modernize Aluminum Alloy Casting Processes

927D0103A Moscow LITEYNOYE PROIZVODSTVO in Russian No 10, Oct 91 pp 6-7

[Article by M.D. Tikhomirov, D.Kh. Sabirov, and A.A. Abramov, Central Scientific Research Institute of Metallurgy]

UDC 621.74:669.001.63:681.3

[Abstract] Because modern casthouses do not have enough highly trained process engineers with extensive design experience, new casting processes are generally developed by the trial-and-error method under actual industrial conditions. This practice adds significantly to the time and money required to develop a finished technology. In an effort to improve this situation, the Central Scientific Research Institute of Metallurgy [TsNIIM] developed the Poligon application package for use in working out several of the most important casting process parameters on a model of the casting process on IBM XT or AT-type PC's. The Poligon application package is intended to analyze the solidification process and its effect on the development of strains during the hardening period. The Poligon application package may be used to work out the following parameters: casting geometry and shape, thin paint coatings on the surfaces where mold and casting meet, type of alloy required, mold materials (up to nine different materials may be used in a mold simultaneously), initial temperature distribution throughout the mold and molten metal, pressure under the heel, and temperature of the surrounding environment. Preparation of data for use with the application package has been maximally automated, and a special graphic editor is used. The algorithms and source data base are oriented primarily toward casting aluminum alloys in a chill mold but may also be used for other alloys and other casting techniques. The packs feature an advanced user service and friendly interface. The Poligon application package has been designed in accordance with a modular principle, with each module having the capability of operating independently or together with the others as a unified package. Eight programs are included in the Poligon package: Molniya [lightning] is a program for express calculation of the solidification time of the different elements of a casting, Tranzit [transit] is a program to send graphic information from sketches created in an AutoCAD system into the files used by the Poligon package, Evklid [Euclid] is used to create a geometric image of the analysis object in the form of vector contours, Diskret [Quantum] is used to prepare the computation grids required for numerical computations, Furye [Fourier] is used for numerical computation of the solidification process, Paskal [Pascal] is used for numerical computation of the feed process, Guk [Hooke] is used to make numerical strain calculations, and Mirazh [Mirage] permits independent visualization of computation results. The Poligon application package is slated for modification to permit its use in the following tasks: solving a two-dimensional strain program (this program will be implemented at the end of 1991), solving the problem of filling a mold to calculate the initial temperature distribution in a casting, and automating the process of optimizing process parameters. Work to expand the Poligon application package's data base is also under way.

Commercial Production of Aluminum Granules for Use in Ferrous Metallurgy

927D0102G Moscow TSVETNYYE METALLY in Russian No 11, Nov 91 pp 61-63

[Article by V.V. Belyayev, I.V. Volkov, V.G. Gopiyenko, B.P. Nazarov, A.I. Palenko, Ye.D. Slovokhotov, V.G. Uvarov, and V.P. Cherepanov, All-Union Scientific Research and Design Institute of the Aluminum, Magnesium, and Electrode Industry and the Volgograd Aluminum Plant]

UDC 669.715

[Abstract] The All-Union Scientific Research and Design Institute of the Aluminum, Magnesium, and Electrode Industry [VAMI] has developed four equipment sets/process flows for use in producing granulated aluminum from melts. Three have already completed the commercial development stage, two of the three have been

introduced at the Volgograd Aluminum Plant, and the third has been introduced at the Klyuchevsk Ferroalloy Plant. The first equipment set/process flow, which is now in operation at the Volgograd Aluminum Plant, entails free or vibratory pouring following by cooling in fluid, drying, and classification. It is designed to produce disk-shaped lenticular granules measuring 3 to 20 mm in size and weighing 0.5 to 1.5 g. The equipment set/process flow has a capacity of 0.2 to 1.0 t/h, results in granules of stable size and shape, and may be used in killing steel, in carburizing gallium from aluminate solutions, and in the chemical industry. Its major drawbacks are contact between the granules and flue, the need for drying, and a low cooling rate. The second equipment set/process flow (which has not yet been introduced at a commercial plant) entails free or vibratory pouring plus cooling on a cold surface. It is designed to produce hemispheric and lobe-shaped granules measuring 5 to 40 mm and weighing 0.5 to 1.5 g at a rate of 0.1 to 2.0 t/h. Its advantages include the fact that the granules do not come into contact with fluid, no drying is required, cooling is rapid, and it may be used to granulate chemically active alloys. It may also be used to kill steel, carburize gallium, as well as produce chemicals, intermediate products for grinding, foundry alloys, rolled sheets, and pigments. Its major drawback is that it results in granules with a size and shape that make them ill-suited for mechanical working. The third equipment set/process flow (which has been introduced at the Volgograd Aluminum Plant) entails centrifugation of a melt plus cooling in fluid, drying, and classification. It is designed to produce spheroidal and lobe-shaped particles weighing 0.002 to 0.05 g in three sizes (0.2 to 2.0 mm, 1.0 to 3.0 mm, and 1.0 to 5.0 mm) at a rate of 0.6 to 2.5 t/h. It is highly adaptable from the standpoint of the size and structure of the granules produced and features a high cooling rate; its disadvantage is that the granules come into contact with fluid and must be dried. It may be used to powder substitutes and pigments and may also be used for killing steel, aluminothermy, and powder metallurgy. The fourth equipment set/process flow (which has been introduced at the Klyuchevsk Ferroalloy Plant) is designed to produce needlelike, spindle-shaped, and lobe-shaped granules weighing 0.002 to 0.06 g with diameters of 0.2 to 2.0 mm and lengths of 3 to 10 mm at a capacity of 0.6 to 1.0 t/h. It may be used in aluminothermy, killing steel, and powder metallurgy, as well as to produce foundry alloys, pigments, and powder substitutes. Its major drawback is the large collecting tank required, the intense heat regimen required, and low cooling speed. Its major advantage is that the granules do not come into contact with fluid and do not need to be dried. All of these equipment sets/process flows appear quite promising. The major drawback to the wide-scale commercial development of production of aluminum granules remains the unjustifiably low price of aluminum granules. Until the price commanded by aluminum granules rises, further progress in the production of granulated aluminum for use in ferrous metallurgy is impossible. Figures 4, tables 2

The Effect of Duration of Annealing on the Mechanical Properties of Aluminum Tubes

927D0102F Moscow TSVETNYYE METALLY in Russian No 11, Nov 91 p 60

[Article by Yu.S. Dodin, V.K. Galayev, and S.A. Zolotarev, Novomoskovsk affiliate, Moscow Chemical Technology Institute imeni Mendeleyev]

UDC 621.77.04.001

[Abstract] The aluminum tanks, tubes, and vessels that are now widely used to package different types of products are made from flat cylindrical blanks (rondels). The process used to produce finished products depends largely on the mechanical properties of the aluminum used. The authors of this concise report examined the effect that duration of annealing has on the mechanical properties of rondels made of A7 aluminum. The rondels studied had a hardness of 35.7 after rolling and cutting and an ultimate rupture strength of 110 MPa. After holding at a temperature of 530-550°C for 10, 20, and 30 minutes, specimen rondels were determined to have had Brinell hardness values of 18.0, 18.1, and 17.7, respectively, and respective ultimate rupture strengths of 71.5, 70.0, and 71.8 MPa. Holding for 10 minutes was thus deemed sufficient to eliminate the workhardness developed during rolling and cutting. Figure 1; references 3 (Russian).

Pressing Aluminum Profiles for the Automotive Industry

927D0102E Moscow TSVETNYYE METALLY in Russian No 11, Nov 91 pp 57-59

[Article by L.S. Skoblov, Avtoprommaterialy Scientific Production Association of the Automotive Materials Scientific Research Institute]

UDC 669.715.018.8/669-421-126

[Abstract] Pressed aluminum sections are used in the autotrains, automobiles, and buses produced at a number of plants, including the Minsk and Kamsk Automotive Plants, the Mytishchi Machine Building Plant, and the Belarus Automotive Plant. Although shaped sections of virtually any configuration can be produced by pressing, the technical and economic feasibility of the production of shaped sections is restricted to a list of products falling within ranges established for such parameters as overall dimensions and the ratio of the thicknesses of various components. Several classifications of types of shaped sections that make it possible to estimate the complexity of manufacturing such sections have been published elsewhere. These complexity ratings must be taken in consideration when designing new shaped sections for inclusion in motor vehicles because complexity of manufacture is a major factor in a given product's production costs. Designers must also give careful consideration to the type of alloy to be used

in a given shaped section and to the state in which the shaped sections are to be shipped. The production costs associated with working with individual alloys must be weighed against the performance characteristics of parts made from those alloys. The aluminum alloy D16, for example, results in products with a good mix of high strength, plasticity, elasticity, and other products; however, the fact that it is difficult to deform and shape means that it is only feasible for use in standard or close-to-standard configurations. Analogously, the alloys AV, AK4-1, V95, AMg5, and AMg6, which are widely used in the aviation industry, cannot be recommended for use in the automotive industry either. The alloys AD31, 1915, 1925, and 1935, on the other hand, have a satisfactory mix of performance characteristics and lend themselves to pressing. Although shaped sections from the latter group of aluminum alloys are not as strong as shaped sections made of D16, AK4-1, and V95, they are strong enough for use in bearing structures, including in the automotive industry. AD31 is a medium-strength alloy of the system Al-Mg-Si that is highly suited to pressing. The alloys 1915, 1925, and 1935 (of the system Al-Zn-Mg) differ from one another with respect to their Mg and Zn contents and the amount of impurities they contain; 1925 is virtually pure, whereas 1915 contains significant amounts of Cu, Fe, and Si. Because 1935 contains less magnesium than 1915, shaped sections made of it are about 20% less strong than analogous sections shaped from 1915. The following recommendations must be kept in mind when using AD31, 1915, 1925, and 1935: 1) all are better used in solid profiles than in hollow ones; 2) 1915 and 1925 should be used only for mass-produced solid shaped sections used in highly loaded structures; 3) 1915 may also be used in welded structures in which a significant drop in the strength properties of the weld is not permissible; 4) AD31 is preferred from the standpoint of economy and the weight characteristics of products produced from it; and 5) 1935 is advisable for use in welds of thin-walled hollow sections. Figure 1, table 1; references 9 (Russian)

An Analysis of the Crystallization and Structure Formation of Round Ingots During Continuous Casting of Aluminum Alloys

927D0102D Moscow TSVETNYYE METALLY in Russian No 11, Nov 91 pp 54-57

[Article by A.N. Kuznetsov, V.V. Sobolev, M.P. Borgoyakov, P.M. Trefilov, and A.I. Zhernov, KraMZ (not further identified)]

UDC 669.715.621.74.047

[Abstract] The authors of the study examined the crystallization kinetics and structure formation of round aluminum ingots produced by the technique of continuous casting. Specifically, they performed a mathematical analysis of the solidification of different-diameter D16 and D1 aluminum ingots produced in a continuous mold. The calculations indicated that the structure formation of continuously cast round ingots could be controlled by removing heat from the ingot in the secondary-cooling zone. The depth of the liquid phase and crater were both found to increase as the intensity of heat removal decreased; the mean-integral time for which the ingot was in a two-phase state also increased as heat removal decreased. The structure of the continuously cast aluminum ingots studied was shown to consist mainly of columnar crystals. The main parameters of the study ingots' dendrite structure (the thickness of the first-order axes, which determines grain size, and the distance between the secondary axes of the dendrites) were found by using relationships published elsewhere, as were the relative volume, dimensions, and density of their pores. The parameters of the dendrite structure of the round aluminum ingots studied were found to change in a nonmonotonic fashion through the ingot cross section. Specifically, they increase in the direction from the periphery to the center of the ingot, reach a maximum, and then diminish. The distance between the secondary axes of the dendrites on the surfaces of the liquidus was found to increase as the level of metal in the mold increased owing to the slowing of the cooling rate. The average thickness of the inclusions of excess components and density of the dislocations were also found to change nonmonotonically throughout the ingot cross section, with the average inclusion thickness behaving analogously to the distance between the dendrites' secondary axes and the dislocation density diminishing in the direction from the surface to the center of the ingot, reaching a minimum, and then increasing somewhat closer to the center. The nature of pore formation was found to depend primarily on the axial length of the two-phase zone and on its permeability. Increases in ingot diameter and casting speed were found to result in increases in the length of the two-phase zone, the distance between the dendrites' secondary axes, and the average thickness of the inclusions. These and other calculated results were found to be in good agreement with experimentally obtained data, thus leading the authors to recommend their new analysis method for use in predicting the crystallization kinetics and structure formation of continuously cast round aluminum ingots. Figures 4, references 14 (Russian)

Commercial Permanent Magnets With Rare Earth Metals

927D0102C Moscow TSVETNYYE METALLY in Russian No 11, Nov 91 pp 48-49

[Article by N.K. Frolova, L.A. Dolomanov, Yu.A. Ravkov, I.P. Pazdnikov, Yu.V. Isaichev, and V.P. Povetyev]

UDC 669.85.86.669.018.58

[Abstract] For the past 20 years, a group of researchers and practitioners from the State Scientific Research and Design Institute of the Rare Metal Industry [Giredmet]

and the Giredmet pilot plant in Pyshma have been working on the problems associated with the development and introduction of a technology to produce permanent magnets made of rare earth metals. Specifically, they have studied rare earth metal-cobalt alloys as material for permanent magnets. This research has been concentrated primarily on two compounds, $REMCo_5$ and $REMCo_{17}$. The properties of magnetic materials have been improved by adding additives to the alloys $SmCo_5$ and Sm_2Co_{17}. Complex alloys with small amounts of copper, iron, zirconium, and other elements having a magnetic energy of about 250 kJ/m^3 have also been created. Work has also been conducted in the direction of replacing samarium by mish metal. The development of Nd-Fe-B magnets, which have a magnetic energy up to 350 kJ/m^3, began in 1983. Additional research has since shown that the main drawback of these magnets (i.e., their low Curie temperature) may be remedied by adding cobalt and subjecting them to heat treatment. In 1983-1985 the United States, Japan, and the USSR produced permanent magnets based on $Nd_2Fe_{14}B$. The Giredmet pilot plant in Pyshma is now producing permanent magnets intended to create a magnetic field in the magnet systems of various special-purpose instruments and household devices. Permanent magnets are being produced in the form of plates, disks, rings, and other shapes based on customers' requests. In the USSR rare earth metals have definitely found their niche as materials for permanent magnets. The markets for such magnets depend largely on the cost and availability of the starting materials. The cost of starting rare earth metal alloys suitable for the production of permanent magnets could be reduced considerably (by 20-30%) by using the method of direct reduction from oxides of the respective metals to produce alloy powders. Such a technology has been developed and tested at the Giredmet but has not yet been used commercially. The magnets produced by the proposed process are in no way inferior to sintered magnets and have a maximum energy product of about 300 kJ/m^3. Despite the fact that they are still expensive, rare earth metal permanent magnets can eventually provide a cost savings both in the creation of new instruments and devices and in the fundamental modification of existing instruments. In addition, the costs of producing them will decrease as they begin to be used more widely. Table 1; references 5: 1 Russian, 4 Western.

Ways of Improving the Quality of High-Purity Niobium

927D0102B Moscow TSVETNYYE METALLY in Russian No 11, Nov 91 pp 43-46

[Article by A.V. Yelyutin, Ye.F. Timofeyev, L.I. Voronenko, A.N. Rylov, P.V. Filippov, and V.N. Ustimenko]

UDC 669.28.548.55

[Abstract] The chemical purity and homogeneity of ingots of refractory metals produced by electron beam refining is dictated largely by the stability of the heat conditions of the melting process. The currently used correction of the melt-heating process by regulating the total power expended on melting as monitored by measuring instruments is not sufficiently precise because the useful portion of the power fed to the melt is not constant and does not lend itself to direct measurement. In addition, the optical pyrometry methods generally used to monitor melting in a vacuum yield only extremely approximate results at best. In view of these facts, the authors of the study reported herein worked to develop ways of improving the quality of high-purity niobium by stabilizing the heat conditions of the electron beam melting process. Specifically, they examined the feasibility of optimizing melting process heating conditions and controlling the process of the electron beam melting of niobium based on its measurable rate of vaporization. The melting was implemented by the drop method with periodic drawing of the ingot at a specified rate and periodic feeding of the starting material into the melt at another specified rate. A quartz optical system was used to direct a parallel beam of radiation of the spectrum of niobium over the surface of the melt (at a height of 0.5 m above its surface) from a lamp with a hollow cathode. The spectral line at 407.97 nm with an intensity of I_0 was isolated. An MDR-23 monochromator or FVN05 narrowband interference filter was used as a dispersing element. The vaporization of the metal as it entered the crystallizer was measured by the attenuation of I_0. A series of expressions were developed for use in calculating the amount of absorption and for linking the optical density of the metal's atoms with its rate of vaporization. An experiment using four specimens of niobium weighing 1.5 kg each was conducted to verify the validity of the expressions. The calculated and experimentally obtained results were found to be in good agreement with one another. The experiments performed confirmed that the atomic absorption method may indeed be used as a basis for automatic control of the process of the melting of a metal such as niobium by regulating the rate or power of the melting process based on continuous measurement of the niobium vaporization rate by means of a special small analyzer functioning as a transducer in an automated control system. Figures 2, table 1; references 5 (Russian).

Dependence of Sb Solubility in Slag on Temperature and Slag Contents

927D0030B Moscow TSVETNYYE METALLY in Russian No 6, Jun 91 pp 23-25

[Article by M.L. Sorokin, S.A. Laykin, V.Ya. Zaytsev, I.I. Kirillin, and D.K. Donskikh, Moscow Institute of Steel and Alloys, and Kadamdzhay Antimony Making Combine]

UDC 669.753.1

[Abstract] An experimental study of Sb solubility in slag was made on slag containing 38.89% metallic Fe and

34.67 % Fe^{2+} ions along with 29.45 % SiO_2, 4.38 % CaO, and 10 % Na_2O. This slag was held in sealed 100 cm^3 capacity quartz flasks under vacuum, together with 2 g of metal and 4 g of synthetic slag in an alundum crucible as well as with 140 mg of $CaCO_3$ as gas source. These flasks, upon removal from a furnace and subsequent cooling in air, were analyzed in an LKhM-8 chromatograph for CO_2 and CO contents in the gaseous phase. The oxygen pressure in them was determined from the ratio of CO_2-pressure to CO-pressure. The content of the solid phase was determined on the basis of chemical and mineralogical analyses. Regression and dispersion analyses of the data based on the Wagner-Chipman model, taking into account equilibrium of the two reversible reactions [$3FeO + CO_2 \rightarrow Fe_3O_4 + CO$; $Fe_3O_4 + CO \rightarrow 3FeO + CO_2$] and [$4FeO \rightarrow Fe_3O_4 + Fe$; $Fe_3O_4 + Fe \rightarrow 4FeO$], indicate that this model is adequate at a P = 0.95 confidence level with a R = 0.84 correlation coefficient. The results reveal how Sb solubility depends on the CaO, Na_2O, SiO_2, and Fe content. It decreases as the amount of SiO_2 or Na_2O is increased and increases as the amount of Fe is increased. Its dependence on the CaO content is nonmonotonic with an extremum: Sb solubility peaking to a maximum (4 atom.%) as the CaO content is increased from 4.3 % to 9 %, with attendant increase of the Sb content in the slag and decrease of the Fe content in precipitated metallic Sb. Substitution of up to 42 % Fe for any of the three CaO, SiO_2, Na_2O slag components will raise the Sb solubility up to 35 % Sb. Figures 3; tables 1; references 9.

Producing Polycrystalline Silicon With a Reduced Microimpurity Content

927D0102A Moscow TSVETNYYE METALLY in Russian No 11, Nov 91 pp 38-40

[Article by E.P. Bochkarev and S.Sh. Kalantaryan]

[Abstract] The semiconductor polycrystalline silicon that is now being mass-produced is inadequate for use in many new-generation semiconductor instruments. The process of hydrogen reduction of trichlorosilane in core-type metal reactors presently remains the main process used to produce polycrystalline silicon. The trichlorosilane, hydrogen, and materials used to construct the process equipment are all sources of possible contamination of silicon produced by the said technique. The graphite used to manufacture the components used to secure the silicon cores and the stainless steel used to construct the reactor are especially important sources of impurities. In view of these facts, the authors of the study reported herein worked to develop a series of measures to increase the purity of polycrystalline semiconductor silicon produced by hydrogen reduction of trichlorosilane in a core-type device. First, to remove suspended particles, the trichlorosilane was subjected to conventional rectification cleaning and then to thermal distillation (film rectification with the application of a temperature field to the vapor), which is more effective than conventional rectification. The thermal distillation device (which was made of nickel) was also used as a trichlorosilane evaporator to make the starting hydrogen-chlorosilane mixture. The thermal distillation was conducted in an incomplete evaporation mode: The impurity-enriched portion of the liquid trichlorosilane (10% of the starting trichlorosilane fed) was continuously removed from the cube and diverted for additional rectification cleaning. Additional filtration on fluoroplastic (F-42) microfilters with a pore size of 0.08 μm was used to remove aerosol impurities from the hydrogen to be used in the silicon production process. The graphite components of the reaction equipment were subjected to chemical and heat treatment after being manufactured. Special measures were also taken to ensure the purity of the polycrystalline silicon produced in the 24-core nickel apparatus used. Specifically, the content of electrically active impurities was determined by photoluminescence analysis, the content of metal impurities was determined by the neutron-activation method, and the content of carbon and oxygen was determined by the method of activation by He^{+3} ions. An indirect method based on measurement of the resistivity of control monocrystals after 1 and 10 passes through the reaction zone was also used. Comparisons of 22 control batches of polycrystalline silicon produced in the usual manner with test batches produced by using the modified process confirmed that the purity improvement measures taken did indeed result in polycrystalline silicon with improved electrophysical parameters. As a result of the studies performed, the authors recommended adoption of their proposed measures. Table 1; references 7: 5 Russian, 2 Western.

A Diffusion-Dispersion Method of Hardening the Surface of Austenite Steel

927D0105A Moscow METALLOVEDENIYE I TERMICHESKAYA OBRABOTKA METALLOV in Russian No 11, Nov 91 pp 2-4

[Article by V.I. Belyakova, A.A. Vereshchagina, and I.P. Banas, All-Union Scientific Research Institute of Aviation Materials Scientific Production Association]

UDC 621.785.5:669.14.018.8

[Abstract] A new diffusion-dispersion method of hardening the surface of austenite steel has been developed that makes it possible to greatly increase the thickness of the hardened layer. Conventional nitriding of austenite steels is generally performed in the temperature interval from 500 to 700°C. The new method, on the other hand, is based on carburizing and carbonitriding at higher temperatures (950 to 1,050°C). The new method results in high-strength layers up to 1 mm thick (as opposed to the layer thicknesses of 0.1 to 0.2 mm) generally achieved when austenite steels are subjected to conventional nitriding. After subsequent heat treatment, the layers produced by using the new method had a hardness of up to 700 HV. In essence, the new diffusion-dispersion method entails diffusion saturation of corrosion-resistant austenite steel with carbon or carbon and nitrogen in a gradual regimen. A hardened surface layer is produced primarily by the release of special carbides during aging. After being subjected to the new diffusion-dispersion method, specimens of 25Cr18Ni8W steel were found be stronger, more resilient, and more resistant to fatigue during bending and wear than specimens subjected to conventional nitriding. The test specimens proved stronger and more durable than the control specimens through the temperature interval from 20 to 300°C. In addition, the specimens subjected to the new surface hardening technique were found to possess satisfactory corrosion resistance in a chamber simulating tropical conditions after a layer 0.1 to 0.15 mm had been ground off. Figures 4, table 1.

Development and Commercial Use of a High-Frequency Current Regimen of Heating the Head of Rails Made of Hypereutectoid Steel

927D0105C Moscow METALLOVEDENIYE I TERMICHESKAYA OBRABOTKA METALLOV in Russian No 11, Nov 91 pp 6-8

[Article by D.K. Nesterov, N.F. Levchenko, V.Ye. Sapozhkov, and V.A. Dubrov]

UDC 621.785.545:669.14.018.294.2

[Abstract] The Ukraine Metals Scientific Research Institute has developed a technology for combined heat treatment of rails made of hypereutectoid steel that entails surface hardening involving high-frequency current heating of the rail heads after they have first been subjected to cyclic spheroidizing annealing to produce a granular perlite structure. The new process was used as the basis for developing a high-frequency current heating regimen for rail heads at the Azovstal Metallurgy Combine. The studies performed indicated that high-frequency current heating of the rail heads made of steel with a granular perlite starting structure at a rate of or about 10°C/s within the temperature interval from 880 to 950°C results in hardness values of 61 to 64 HRC and ultimate strength values of 1,430 to 1,440 N/mm^2 with a high plasticity and impact strength. Similar treatment of specimens with a plastic perlite starting structure was found to result in lower mechanical properties and hardness values. Specifically, when subjected to high-frequency current heating at temperatures of 850 to 900°C, specimens with a plastic perlite starting structure were found to attain hardness values of 58 to 61 HRC and an ultimate strength of 1,385 to 1,400 N/mm^2. Batches of rails made of hypereutectoid carbide steel were produced at the Azovstal combine by using the new technology. The rails were found to possess a good set of mechanical properties (ultimate strength, 1,370-1,450 N/mm^2; $\sigma_{0.2}$ = 945-1,050 N/mm^2; δ_5 = 9.6-12.5%, ψ = 34-37%; and a_1 = 32-41 J/cm^2). Batches of rails weighing 350 tons are now undergoing performance tests under the especially severe conditions of the Far North. Figures 2, tables 3; references 2 (Russian).

Improving the Characteristics of the Shape Memory Effect of Copper Alloys by Optimizing the Heat Treatment Regimen

927D0105E Moscow METALLOVEDENIYE I TERMICHESKAYA OBRABOTKA METALLOV in Russian No 11, Nov 91 pp 35-38

[Article by G.Z. Zatulskiy, M.A. Kravchenko, V.K. Larin, and A.M. Firsov, Kiev Polytechnic Institute and Leningrad Shipbuilding Institute]

UDC 621.785:669.2/8.01.7

[Abstract] The authors of this article have reviewed existing processes of heat-treating copper-based alloys with a thermoelastic martensite transformation. Specifically, they concentrate on alloys of the systems Cu-Al-Zn, Cu-Al-Mn, and Cu-Al-Ni. The following are the main conclusions of their literature review. To date, a great many studies have taken the conventional single-factor approach to optimizing heat treatment regimens. The approach of a multifactoral experiment based on the theory of mathematical planning of scientific research would be far a more effective approach to optimizing the heat treatment regimens of copper alloys with a shape memory effect for a number of reasons. Fewer tests and less time would be required, and the effect of uncontrollable factors would be minimized. Some research based on the multifactoral experiment approach has been conducted on the heat treatment of alloys of the system Cu-Al-Mn. The following were specified as primary factors when the experiment was planned: chemical

composition of the alloys, rate of cooling during crystallization, annealing temperature and time with cooling in air, temperature of heating during hardening, holding, and hardening medium. Because heterogenization of test alloys' structure and consolidation of their components have a negative effect on their subsequent treatment and properties, high-temperature annealing followed by slow cooling is clearly unsuitable for copper alloys with a shape memory effect. For this reason, normalization must be included as the first stage of heat treatment in the plan of a multifactoral experiment. The ranges in which each of the aforesaid factors are sought, as well as the levels of their variation, are determined by literature data and on the basis of preliminary experiments conducted prior to the main experiment. To find the optimal heat treatment technology, it is necessary to generate a plan of the type $2^1 \times 3^2 \times 4^4 \times 8^1/64$, which will result in an effectiveness of obtaining useful information from 64 experiments reaching 99.6%. The regression models constructed in the form of orthogonal Chebyshev polynomials are optimized together based on the response maxima. As responses, it is necessary to select those characteristics of the shape memory effect that are most dependent on the nature of the alloy rather than the conditions of the experiment, namely, reactive stress and ultimate strain. Heat treatment regimens determined in this manner would make it possible to improve the heat treatment properties of given alloys individually. Although studies performed on different bronze specimens indicate that heat treatment regimens tailored to individual alloys result in different structure and phase composition changes in individual alloys, it has been possible to identify several changes that are commonly experienced by alloys with a shape memory effect and that thus may be linked to an intensification of the shape memory effect. Specifically, the parameters of the martensite transformation of medium- and high-manganese bronzes have been found to remain rather stable with respect to two-stage heat treatment, whereas two-stage heat treatment of low-manganese bronzes results in a significant redistribution of alloy-forming elements and in an unacceptably large displacement of the characteristic temperatures of the martensite transformation (by 40 to 80°C). Tables 2; references 20: 13 Russian, 7 Western.

Effect of Grain Size and Duration of Low-Temperature Tempering on the Properties of Tool Steel

927D0105F Moscow METALLOVEDENIYE I TERMICHESKAYA OBRABOTKA METALLOV in Russian No 11, Nov 91 pp 42-43

[Article by B.S. Natapov, Zaporozhye Machine Building Institute]

UDC 620.14.018.25

[Abstract] Despite the large number of works that have been devoted to the mechanical properties of carbon tool steels, several questions regarding the strength of such steels still remain open. One such question is the possibility of increasing the strength of tool steel by creating a fine grain and increasing the duration of low-temperature tempering. Research published elsewhere indicates that increasing grain size from 15 to 100 μm reduces tear resistance from 1,500 to 700 N/mm^2. According to other published data, hardening and tempering at 200°C results in an ultimate strength of 2,700 and 2,800 N/mm^2 in U8 steel with a grain size of 1 to 3 μm. Research conducted by the author of this article back in 1945 established that increasing the duration of tempering to more than 3.5 hours increases the ultimate strength of U8 steel to 2,500-2,600 N/mm^2 while reducing hardness from 64 to 60 HRC. In the case of type 45 steel, the same duration of tempering results in an ultimate strength of 2,040 N/mm^2 with a plasticity of 48%. Low-temperature (150-250°C) tempering has also proved to be important in increasing the mechanical properties of tool steels with different carbon contents. Figures 2; references 7 (Russian).

Laboratory Unit for Diffusion Welding in Glow Discharge

927D0096 Kiev AVTOMATICHESKAYA SVARKA in Russian No 12, Dec 91 (manuscript received 14 May 91) p 65

[Article by G.P. Bolotov, candidate of technical sciences, Chernogolovka Technology Institute]

UDC 621.791.4.03:539.378.3:537.525

[Abstract] Diffusion welding is becoming increasingly more popular as a way of joining materials. The use of the technique is limited, however, by the fact that existing diffusion welding equipment is designed for operation in a vacuum of at least 1×10^{-2} to 1×10^{-3} Pa, which in turn necessitates the use of large and costly equipment. A new unit for diffusion welding in a glow discharge has been developed. The big advantage of using a glow discharge is that significantly higher pressures (1×10^{2} to 1×10^{4} Pa) may be used. Another important benefit of the new diffusion welding unit is that no compression system is needed. This is because the required compression of workpieces is accomplished in a rigid closed force loop by thermal tension. The current source for the glow discharge includes a thyristor voltage regulator, a step-up transformer, and a rectifier. Thermocouples and a millivoltmeter are used to control the heating temperature. The main technical characteristics of the new unit are as follows: supply system voltage, 38 V; power requirement, 5 kW; discharge power, 0 to 3 kW; maximum heating temperature, 1,273 K; compressive force, 0 to 10 kN; ultimate rarefaction, 10 Pa; working gas pressure, 0 to 13.3 kPa; weight, 160 kg; and overall dimensions, 1,000 x 650 x 1,700 mm. The new unit may be used to join components up to 20 mm in diameter and up to 150 mm high. Figures 2; references 2 (Russian).

A Technology and Device To Joint Thermoplastics With Metal and Nonmetal Materials

927D0096E Kiev AVTOMATICHESKAYA SVARKA in Russian No 12, Dec 91 (manuscript received 6 Mar 91) pp 60-61

[Article by V.P. Tarnogrodskiy, candidate of technical sciences, and Ye.Yu. Ponomareva, engineer, Electric Welding Institute imeni E.O. Paton, Ukraine Academy of Sciences]

UDC 621.791.46:678.029.43

[Abstract] Because thermoplastics cannot be welded to other materials, they are most frequently joined to metal and nonmetal materials by bolting or riveting. Thermoplastic rivets are forced by a heated tool or by an ultrasound waveguide, which requires significant material and equipment expenditures. In view of these facts, specialists from the Electric Welding Institute imeni E.O. Paton worked together with the GosdorNII [not further identified] to develop a device and process to connect thermoplastics with different materials and to create a strong joint in the process. A heated tool that has a semicircular groove is moved along the entire perimeter at the level of the plane of the joint of the two materials. The heated tool may have any type of cross section and is made of a heat-conducting material such as aluminum, copper, brass, or steel. The tool's working surface, which may be heated by any energy source, is covered with an antiadhesive layer. The semicircular groove present on the heater permits the formation of a thickening (bead) of coagulated thermoplastic. When the heater (heated tool) is removed, the bead slides elastically thanks to the elasticity of the heated material and the smoothness of the groove. The bead formed strengthens the joint against shearing and breaking. The depth of the semicircular groove should be about one-sixth the diameter of the heater (the reasons why this depth is optimal are explained in detail). The new device has been used successfully to join polyvinyl chloride and polystyrene as well as join low-pressure polyethylene with aluminum. Experiments have demonstrated that the new method of forming a thermoplastic bead increases the strength of thermoplastic joints by about a factor of 2. Figures 3; references 2 (Russian).

The Effect of the Composition and Structure of Complexly Doped Fe-Based C-Cr-Nb Alloys on Their Resistance to Impact and Abrasive Wear

927D0096D Kiev AVTOMATICHESKAYA SVARKA in Russian No 12, Dec 91 (manuscript received 28 Mar 90; after revision 11 Jun 91) pp 43-45

[Article by V.M. Mozok, candidate of technical sciences, A.I. Danilets and L.P. Kryzhanovskaya, engineers, Electric Welding Institute imeni E.O. Paton, Ukraine Academy of Sciences, and I.M. Spiridonova, doctor of technical sciences, and G.V. Zinkovskiy, engineer, Dnepropetrovsk State University]

UDC
[621.791.92:669.15'26'293'295.018.25:620.18]:539.538

[Abstract] The authors of the study reported herein examined the effect of the composition and structure of complexly doped iron-based carbon-chromium-niobium alloys on their resistance to impact and abrasive wear. Specifically, 11 alloys with the alloying system Fe-C-Cr-Nb-Ti and process additives were tested in the wear resistance laboratory of the Electric Welding Institute imeni E.O. Paton. The said alloys were applied to specimens of St3 steel in two layers in a regimen entailing an arc current of 300-340 A, arc voltage of 30-32 V, electrode tip of 60-70 mm, and surfacing rate of 8-10 m/h. Specimens (measuring 16 x 16 x 6 mm) were cut from the surfaced steel specimens and tested on an OB-959 test stand. Quartz sand with a grain size of 0.2 to 0.8 mm was used as an abrasive material. An impact energy of 4.5 J and an impact velocity of 0.5 m/s were used in the impact wear tests. Each of the specimens was

subjected to a battery of x-ray crystallographic studies and microhardness tests. The studies performed enabled the researchers to establish a link between microstructure and resistance to abrasive and impact wear. Specifically, those specimens that had a predominantly austenite or austenite-martensite matrix with a eutectic component based on doped chromium carbide, i.e., Cr_7C3 and $Cr_{23}C_6$, were found to be the most resistant to abrasive and impact wear. On the basis of the studies performed, the authors recommended two alloys for use as filler materials. The first contained the following (% by mass): C, 1.9; Cr, 6.9; Nb, 3.9; Ti, 1.55; Ni, 0.5; and Mo, 2.78. The second alloy recommended contained the following (% by mass): C, 2.8; Cr, 14.7; Nb, 6.00; Ti, 1.60; and Ni, 0.6. The two alloys were found to have a relative wear resistance of 9.27 and 9.24, respectively, and an HRC of 65.6 and 57.1, respectively. Figure 1, tables 2; references 3: 2 Russian, 1 Western.

09KhG2SYuCh Extrastrong Cold-Resistant Steel for Welded High-Pressure Vessels

927D0096C Kiev AVTOMATICHESKAYA SVARKA in Russian No 12, Dec 91 (manuscript received 10 Jan 91; after revision 25 Apr 91) pp 37-42

[Article by S.V. Yegorova, candidate of technical sciences, A.V. Yurchishin and Ye.N. Solina, engineers, A.I. Krendeleva, candidate of technical sciences, and V.M. Kozulin, N.G. Zotova, and N.I. Varenko, engineers, Electric Welding Institute imeni E.O. Paton, Ukraine Academy of Sciences]

UDC 621.791.011:669.15.018.4:621.772

[Abstract] A 1990 article reported the development of the cold-resistant weldable steel 09G2SYuCh, which was developed at the Electric Welding Institute imeni E.O. Paton as an alternative to the steels 16GS and 09G2S (which are widely used in manufacturing ship hulls). 09G2SYuCh was praised for its high impact strength even after welding and for the high quality and high uniformity of sheets made from it; however, it proved to be only slightly stronger than 09G2S. In view of this fact, the Electric Welding Institute imeni E.O. Paton developed a modification of 09G2SYuCh. The new modification, designated 09KhG2SYuCh, preserves all of the advantages of its predecessor but is much stronger. Studies evaluating the mechanical properties, weldability, and technological feasibility of 09KhG2SYuCh as a material for use in constructing ship hulls have revealed that it is indeed superior to the steels previously used to construct high-pressure vessels such as ship hulls. Specifically, the studies performed confirmed that the steel 09KhG2SYuCh and joints thereof have a high impact strength at temperatures as low as -70°C in specimens with round and sharp notches (specimens of 09KhG2SYuCh steel were found to have a 55% higher yield strength than comparable specimens of 09G2S steel, a 20% longer ultimate strength, and a 70% higher impact strength at -60°C after mechanical aging). The studies also established another important advantage of 09KhG2SYuCh steel, namely, that it may be subjected to electroslag welding without subsequent normalization. On the basis of the studies reported, 09KhG2SYuCh steel has been recommended as a replacement for 09G2S because using 09KhG2SYuCh will result in a 17 to 30% reduction in the amount of metal required to manufacture a comparable product. Furthermore, products made of 09KhG2SYuCh steels will be more reliable than those made of 09G2S and may be produced quicker and less expensively. Figures 6, tables 8; references 3 (Russian).

An Investigation of Residual Welding Stresses in Thin-Walled Elements Made of the Composite Alloy KAS-1A

927D0096B Kiev AVTOMATICHESKAYA SVARKA in Russian No 12, Dec 91 pp 7-11, 36

[Article by V.I. Makhnenko, academician, Ukraine Academy of Sciences, V.R. Ryabov, doctor of technical sciences, N.I. Pivtorak, engineer, and I.S. Dykhno and V.M. Shekera, candidates of technical sciences, Electric Welding Institute imeni E.O. Paton, Ukraine Academy of Sciences]

UDC [621.791.38.053:669-419]:539.4.014

[Abstract] A study was conducted to determine the possibility of using mathematical methods to study the stress-strained state in thin-walled structures made of the composite material KAS-1A. (KAS-1A is a matrix made of an aluminum alloy with reinforcing fibers made of high-strength steel.) Specifically, researchers compared the distribution of lengthwise stresses in a welded panel sheathed in three different ways. In the first (standard) version of the sheathing, the reinforcing fibers in the 1-mm-thick sheathing were arranged crosswise to the direction of the weld in a 3-mm-thick band with lengthwise reinforcement. The second version differed from the first in that the 3-mm-thick band was not used. The third version differed from the first in that the sheathing was reinforced in the direction lengthwise along the weld. The calculated and experimentally obtained values of the local and residual stresses that developed when each of the three versions of sheathing were subjected to heating along their edges and along the midline of the band were found to be in good agreement with one another. The studies performed indicated that when structures made of the composite KAS-1A are welded and/or soldered in the conventional regimens, the level of average residual stresses in the heating zone does not exceed 160 MPa when the reinforcing fibers are arranged crosswise to the weld or 180-200 MPa when the reinforcing fibers are arranged lengthwise along the direction of the weld. The studies further confirmed that increasing the intensity (per-unit-length energy) of heating above the welding/soldering regimen thresholds has little effect on the stress level in the case of a crosswise arrangement of the reinforcing fibers but

results in a noticeable increase in stress level when a lengthwise fiber arrangement is used. Figures 4; references 7: 4 Russian, 3 Western.

Holographic Compensation Method of Measuring the Stress-Strained State of Three-Dimensional Welded Structures

927D0096A Kiev AVTOMATICHESKAYA SVARKA in Russian No 12, Dec 91 (manuscript received 29 Oct 90; after revision 17 Apr 91) pp 1-6

[Article by L.M. Lobanov, corresponding member, Ukraine Academy of Sciences, and V.A. Pivtorak and Yu.I. Onishchenko, candidates of physical and mathematical sciences, Electric Welding Institute imeni E.O. Paton, Ukraine Academy of Sciences]

UDC 621.791:[620.1.08:778:38]

[Abstract] A holographic compensation method has been developed that permits quick determination of the sign and numerical values of the three components of the displacement vector (designated as Δr with a right arrow above the r) specifying the stress-strained state of a three-dimensional welded structure. The three components, designated by the letters u, v, and w with right arrows above them, may be determined by using a single holograph as opposed to the three that are generally required. This greatly simplifies the optical train of the holographic interferometer required and increases the stability of the measurement results. Experimental verification of the proposed measurement method revealed that it results in values of σ (u, v) with a precision of about 0.15 μm and values of σ (w) with a precision of about 0.03 μm. The new method permits real-time compensation of the change in the geometry of the holographic interferometer's optical train resulting from a change in the temperature, etc., of the surrounding environment when the test object is held in the holographic unit for lengthy periods. The most intensive deformation of structures examined by using the new holographic compensation method was determined to occur in the first 24 hours of holding under a load. Figures 6, table 1; references 5 (Russian).

The Technological Efficiency of a Shaking Screen Technology To Enrich Gold-Containing Sands

927D0102H Moscow TSVETNYYE METALLY in Russian No 11, Nov 91 pp 64-66

[Article by O.V. Zamyatin, V.M. Mankov, and V.S. Tomin, Irkutsk State Scientific Research Institute of Rare and Nonferrous Metals (Irgiredmet)]

UDC 662.764:622.27.1

[Abstract] At the present time, about half of the balance of placer gold reserves contain an elevated or significant (>25%) fraction of fine (<0.25 mm) gold. The average size of native gold has dropped to 0.3 mm. A great number of dredges are currently processing gold in which fine gold accounts for ≥45% of the gold present. The standard process of enrichment in sluices with a rigid trapping coating, which is effective in trapping large grains of gold, is little suited for extracting finer grains. Research conducted at the Irgiredmet established that about 77% of all process-related gold losses during sand enrichment are associated with grains of the class >0.1 (0.063) mm. Such gold could be extracted adequately by gravitation methods, but the enrichment technology has not been developed sufficiently. The remaining 23% of gold lost has a grain size of <0.1 (0.063) mm. This gold cannot be extracted by simple gravitation methods given existing equipment. To increase the extraction of gold with a grain size of <0.25, the Irgiredmet worked together with the Ural Scientific Research and Design Department of the Ginalmazzoloto and the Irkutsk Heavy Machine Building Plant imeni V.V. Kuybyshev to develop a shaking screen technology of enriching gold-containing sands. The new technology is slated for use with a significant number of the large dredges of the USSR Glavalmazzoloto [not further identified]. According to estimates, the new process will reduce gold losses in the said dredges by a factor of 1.5 to 2 as compared with losses resulting with the sluice technology. A dredge with a capacity of 250 l (series 250 DM, DS) has been developed for use with the shaking screen technology. The new technology has also been implemented in one of two configurations of the TOK-200K enrichment and transport system (capacity, 200 m^3/h) for the open method of enrichment with separate sand recovery. It has been estimated that the new technology will increase operating costs per cubic meter of sands processed but will reduce the costs of obtaining 1 g of metal. Figures 5.

END OF FICHE DATE FILMED

5 May 1992